

## UPDATED RESURFACING HISTORY OF MARS BASED ON THE NEW GLOBAL GEOLOGIC MAP.

K. L. Tanaka<sup>1</sup>, C. M. Fortezzo<sup>1</sup>, J. A. Skinner, Jr.<sup>1</sup>, T.M. Hare<sup>1</sup>, and S. Robbins<sup>2</sup>, <sup>1</sup>U.S. Geological Survey, 2255 N. Gemini Dr., Flagstaff, AZ, 86001, USA, <sup>2</sup>University of Colorado, Boulder, CO, USA.

**Introduction:** A new global geologic map of Mars has been completed in a digital, geographic information system (GIS) format using geospatially controlled altimetry and image data sets [1]. The map reconstructs the geologic history of Mars, which includes many new findings collated in the quarter century since the previous, Viking-based maps [2] were published, as well as other discoveries that were made during the course of the mapping using the new data sets. The technical approach enabled consistent mapping that is appropriate not only for the map's 1:20,000,000 scale but also for its likely widespread use. Each geologic unit outcrop includes basic attributes regarding identity, location, area, crater densities, and chronostratigraphic age. In turn, units are grouped by geographic and lithologic types, which provide synoptic global views of material ages and resurfacing character for the Noachian, Hesperian, and Amazonian Periods.

**Digital Map Product:** The new global geologic map of Mars at 1:20,000,000 scale [1] has been produced using Esri's ArcGIS software. Map layers are registered to the Mars Global Surveyor's (MGS) Mars Orbiter Laser Altimeter (MOLA) global digital elevation model (DEM) at 463 m/pixel [3]. Mapping efforts relied heavily on morphologic and thermal brightness observations from global mosaics of Mars Odyssey (ODY) mission's Thermal Emission Imaging System (THEMIS) daytime and nighttime infrared images at 100 m/pixel [4]. We applied photogeologic mapping techniques similar to those described in [5-6] to identify and discriminate 44 geologic units (forming ~1300 outcrops) and 11 linear feature types (~3500 individual features mapped). These map layers collectively document major episodes of material emplacement, terrain development, and surface modification.

Units are delineated by primary morphologic, thermal/albedo, and topographic characteristics that we interpret were established during unit emplacement, avoiding, where possible, secondary features resulting from subsequent tectonic and (or) erosional modification (i.e., resurfacing). Each map unit is assigned an age range according to the Martian chronostratigraphic periods and epochs [7-8], as governed by superposition relations and impact crater densities. In addition, the units are grouped into geographic (highland, lowland, transitional, basin, polar, and apron) and lithologic (volcanic and impact) categories.

**Age Dating:** Each Martian chronologic epoch has crater-density defined boundaries that are fit to widely used crater production and chronology functions [9-10].

Crater counts were obtained using two approaches. The first consisted of counts of selected typical unit surfaces for craters as small as 100 m; results from this approach are described in [11]. The other method involved the intersection of the geologic map units with the global crater database of Robbins and Hynek [12] that documents the location, diameter, and other morphologic attributes of >380,000 craters larger than 1 km in diameter.

Overall, these age determinations enabled grouping the units by age, resulting in a chronostratigraphic map (Fig. 1), as well as summaries of the areas (Fig. 2) and resurfacing rates (Fig. 3) for each unit group by epoch. Areas and rates are calculated on an age-based scheme that relies on model chronologies. Here, we show example results using the Neukum chronology function, but we have also calculated results based on the Hartmann function. (More results are shown in [13].)

**Chronostratigraphic Map Summary (Fig. 1):** Noachian-aged outcrops (46% of total surface area) dominate exposures of ancient highland terrain on Mars with relatively minor input from volcanic and basin materials. Some isolated Noachian outcrops are still present within the northern lowlands, despite later resurfacing by later activity. Crater preservation as a function of age and terrain indicates that fluvial erosion and local infilling such as by sedimentation and volcanism were dominant Noachian resurfacing processes [14].

Compared with [2], collective mapping results for Hesperian surfaces (22% areal coverage) are similar but many details differ. Exposed Hesperian rocks infill the northern lowlands and large impact basins and form the earliest polar deposits and major extents of the Tharsis and Elysium volcanic rises. Parts of the highland boundary retreated, and canyons and chaotic terrain formed by tectonism, incision, and collapse in Valles Marineris and nearby highland areas. Scattered Hesperian impact craters, which are not discriminated from Amazonian ones, dot the highland landscape.

The Amazonian (32% areal coverage) included continued volcanism in the Tharsis and Elysium regions and local mass-wasting and accumulation of sediments along the highland-lowland transition region. Also, aprons formed around Olympus Mons and Tharsis Montes. Remnants of a Middle Amazonian lowland unit [15] and other basin and volcanic materials cover large patches of the northern plains. A proportion of the scattered outcrops of impact material in the highlands are Amazonian age. The polar plateaus largely formed at this time.

**Updates on Resurfacing History (Figs. 2 and 3):**

We find that Noachian highland surfaces overall have high percentages of their areas now dated as an epoch older than in the Viking mapping [2] (with consequently modified resurfacing rates of those reported by [16]). Pristine impact craters  $\geq 3$  km in diameter occur in greater density on (1) Hesperian terrain (which is volcanically rich) and (2) in a vast Amazonian and Hesperian volcanic unit. This contrasts with their deficit on heavily cratered and otherwise softened Noachian terrain. These

observations are likely due to the relatively stronger, less-impacted yet lava-rich materials making up the younger units. Reconstructions of resurfacing of Mars by its eight geologic epochs using the Hartmann and Neukum chronology models indicate high rates of highland resurfacing during the Noachian, modest rates of volcanism and transition zone and lowland resurfacing during the Hesperian, and low rates of mainly volcanic and polar resurfacing for the Amazonian (Fig. 3).

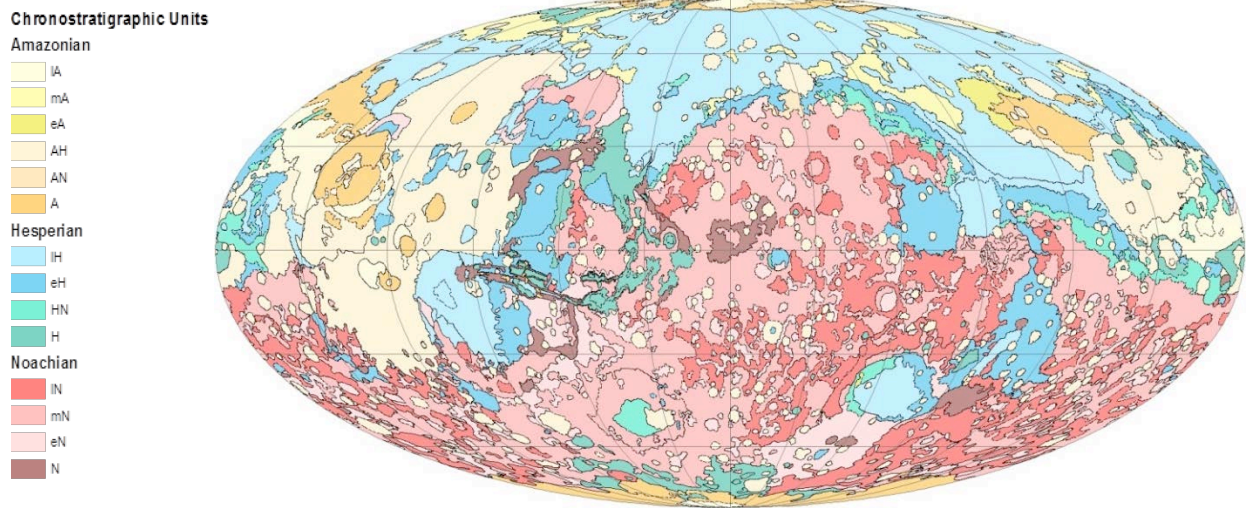


Figure 1. Chronostratigraphic map of Mars. Some units span multiple epochs or periods.

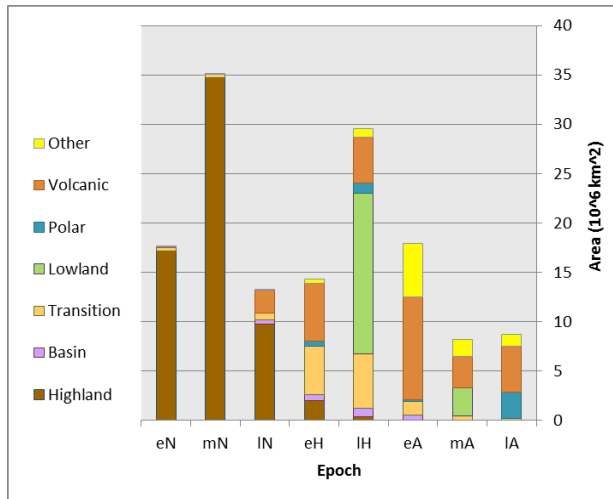


Figure 2. Resurfaced areas on Mars per unit group and epoch, Neukum chronology model.

**References:** [1] Tanaka K.L. et al. (in review) *USGS SIM*. [2] Scott D.H. et al. (1986-87) *USGS Map I-1802-A-B-C*. 004. [3] Smith D.E. et al. (2001) *JGR*, 106, E10. [4] Edwards C.S. et al. (2011) *JGR*, 116, E10008. [5] Tanaka K.L. et al. (2005) *USGS SIM-2888*. [6] Tanaka

K.L. and Fortezzo C.M. (2012) *USGS SIM-3177*. [7] Scott D.H. and Carr M.H. (1978) *USGS Map I-1083*. [8] Tanaka K. L. (1986) *JGR*, 91, E139-E158. [9] Hartmann W.K. and Neukum G. (2001) *Space Sci. Rev.* 96, 165–194. [10] Werner S.C. and Tanaka (2011) *Icarus*, 215, 603-607. [11] Platz T. et al. (in review) *Icarus*. [12] Robbins S. J. and Hynek B. M. (2012) *JGR*, 117, E05. [13] Tanaka K.L. et al. (in review) *PSS*. [14] Irwin R.P. III et al. (in review) *JGR-Planets*. [15] Skinner J.A. Jr. et al. (2012) *Geology*, 40, 1127-1130. [16] Tanaka K.L. et al. (1988) *PLPS XVIII*, 665-678.

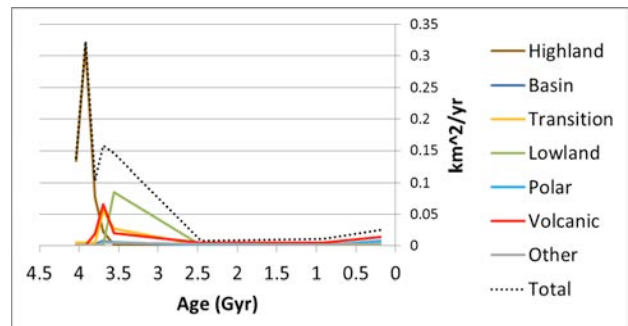


Figure 3. Resurfacing rates on Mars per unit group and mean age of epoch, Neukum chronology model.